The American Journal of Pathology, Vol. 184, No. 4, April 2014

ELSEVIER

The American Journal of
PATHOLOGY
ajp.amjpathol.org

VASCULAR BIOLOGY, ATHEROSCLEROSIS, AND ENDOTHELIUM BIOLOGY

Hematological, Hepatic, and Retinal Phenotypes in Mice Deficient for Prolyl Hydroxylase Domain Proteins in the Liver

Li-Juan Duan, Kotaro Takeda, and Guo-Hua Fong

From the Center for Vascular Biology, Department of Cell Biology, University of Connecticut Health Center, Farmington, Connecticut

Accepted for publication December 30, 2013.

Address correspondence to Guo-Hua Fong, Ph.D., Center for Vascular Biology, University of Connecticut Health Center, 263 Farmington Ave., Farmington, CT 06030-3501. E-mail: fong@nso2.uchc.edu.

Prolyl hydroxylase domain (PHD) proteins catalyze oxygen-dependent prolyl hydroxylation of hypoxia-inducible factor 1α and 2α, tagging them for pVHL-dependent polyubiquitination and proteasomal degradation. In this study, albumin Cre (Alb^{Cre})—mediated, hepatocyte-specific triple disruption of *Phd1*, *Phd2*, and *Phd3* (*Phd(1/2/3)*hKO) promoted liver erythropoietin (EPO) expression 1246-fold, whereas renal EPO was down-regulated to 6.7% of normal levels. In *Phd(1/2/3)*hKO mice, hematocrit levels reached 82.4%, accompanied by severe vascular malformation and steatosis in the liver. In mice double-deficient for hepatic PHD2 and PHD3 (*Phd(2/3)*hKO), liver EPO increase and renal EPO loss both occurred but were much less dramatic than in *Phd(1/2/3)*hKO mice. Hematocrit levels, vascular organization, and liver lipid contents all appeared normal in *Phd(2/3)*hKO mice. In a chronic renal failure model, *Phd(2/3)*hKO mice maintained normal hematocrit levels throughout the 8-week time course, whereas floxed controls developed severe anemia. Maintenance of normal hematocrit levels in *Phd(2/3)* hKO mice was accomplished by sensitized induction of liver EPO expression. Consistent with such a mechanism, liver HIF-2α accumulated to higher levels in *Phd(2/3)*hKO mice in response to conditions causing modest systemic hypoxia. Besides promoting erythropoiesis, EPO is also known to modulate retinal vascular integrity and neovascularization. In *Phd(1/2/3)*hKO mice, however, neonatal retinas remained sensitive to oxygen-induced retinopathy, suggesting that local EPO may be more important than hepatic and/or renal EPO in mediating protective effects in the retina. *(Am J Pathol 2014, 184: 1240—1250; http://dx.doi.org/10.1016/j.ajpath.2013.12.014)*

Prolyl hydroxylase domain (PHD) proteins PHD1, PHD2, and PHD3 use molecular oxygen as a substrate to hydroxylate specific prolyl residues in HIF-1α and HIF-2α,[1–3] tagging them for von Hippel—Lindau protein (pVHL)—dependent polyubiquitination and proteasomal degradation.[4] PHD-regulated HIF-α stability is important for multiple processes, including angiogenesis,[5–7] erythropoiesis,[8–10] cardiomyocyte function,[11–13] cell survival,[14] and metabolism.[15] PHD1 and PHD2 also hydroxylate IKKβ, thus regulating the assembly of NF-κB and functions of monocytic cells and proangiogenic macrophages.[16–19] Besides PHDs, a transmembrane prolyl hydroxylase in the endoplasmic reticulum (P4H-TM) may also regulate HIF-α stability.[20,21]

In normal adults, renal interstitial cells are responsible for the bulk of plasma erythropoietin (EPO) and thus play a key role in regulating erythropoiesis and blood homeostasis. Loss or dysfunction of renal interstitial cells due to acute renal injury or chronic kidney disease can lead to EPO deficiency and severe anemia.[22] Normal liver expresses EPO only at very low levels, but possesses latent capacity for EPO expression that can be reactivated by manipulations that lead to hepatic HIF-2α stabilization. For example, hepatocyte-specific *Vhl* knockout in mice resulted in the accumulation of HIF-1α and HIF-2α to high levels, and subsequent studies showed that HIF-2α was responsible for elevated liver EPO expression and polycythemia.[23,24] Other studies have also demonstrated critical roles of HIF-2α in regulating EPO expression.[25,26]

Our research group has previously shown that germline *Phd1* and *Phd3* double knockout leads to increased liver

Supported by the NIH (grant 5R01-EY019721 to G.H.F.).
Disclosures: None declared.

http://dx.doi.org/10.1016/j.ajpath.2013.12.014

EPO expression.[8] In a more recent study, Minamishima and Kaelin[27] showed that more dramatic liver EPO up-regulation can be induced by triple *Phd* knockout, with *Phd1* and *Phd3* knockout being germline null mutations and *Phd2* knockout induced in a hepatocyte-restricted manner. These studies raised the possibility that the liver may be exploited as an alternative source for endogenous EPO production in case of renal failure. Indeed, siRNA-mediated knockdown of hepatic PHD rescued erythropoiesis in mice subjected to 5/6 nephrectomy.[28] Although these findings are highly encouraging, it is not known how the liver itself is affected by PHD deficiency.

In the present study, we examined hematological effects of hepatic PHD deficiency in an established chronic renal failure model,[29–32] and compared blood, vascular, and lipid phenotypes associated with the disruption of different combinations of PHD isoforms in the liver. Hepatic triple deficiency of all three isoforms caused multiple abnormalities, including severe erythrocytosis, vascular malformation, and massive lipid accumulation in the liver. By contrast, mice double-deficient for hepatic PHD2 and PHD3 did not exhibit any of these defects, but yet gained the ability to maintain normal hematocrit (Hct) levels in a chronic renal failure model. These data provide the proof of principle that selective combinations of hepatic PHD isoforms could offer suitable therapeutic targets for maintaining normal blood homeostasis without accompanying vascular malformation or liver steatosis.

Materials and Methods

Mice

All animal procedures were approved by the Animal Care Committee at the University of Connecticut Health Center in compliance with Animal Welfare Assurance. Alb^{Cre} mice, originally generated by the Magnuson Laboratory at Vanderbilt University,[33] were purchased from the Jackson Laboratory (Bar Harbor, ME). The generation and genotyping of floxed and knockout alleles for *Phd1*, *Phd2*, and *Phd3* have been described previously.[5,6,8]

Chronic Renal Failure Anemia

Chronic renal injury was induced by an adenine-rich diet, as described previously.[29–32] In brief, mice were first maintained on normal chow until 8 weeks of age, and then were switched over to an adenine-rich diet (normal chow supplemented with 0.2% adenine) (Harlan Laboratories, Indianapolis, IN) for another 8 weeks. In control groups, mice were continued on normal chow.

Hemolysis by PHZ

Acute anemia was induced in 8-week-old mice by two intraperitoneal injections of phenylhydrazine (PHZ) administered 24 hours apart, at doses of 0 (saline control), 40, 80, or 120 mg/kg for each injection. At 48 hours after the second injection, mice were euthanized for blood collection and liver and kidney tissue isolation.

OIR Model

To examine the effects of oxygen on retinal vascular integrity, neonatal mice were analyzed by the oxygen-induced retinopathy (OIR) model.[34,35] In brief, mice were exposed to 75% oxygen from postnatal day P7 to P12 for phase I, followed by another 5 days under ambient air (P12 to P17) for phase II.

Measurements of Hct, BUN, Hb, and Serum EPO

Blood samples were collected into EDTA-coated microcuvettes (Sarstedt, Newton, NC). Hct and blood hemoglobin (Hb) values were determined with a scil Vet abc blood analyzer (Scil Animal Care, Gurnee, IL). The blood analyzer was periodically calibrated with standards supplied by the vendor. Additional blood samples were collected into non-coated tubes for serum preparation, and serum EPO concentrations were analyzed with an EPO enzyme-linked immunosorbent assay (ELISA) kit (R&D Systems, Minneapolis, MN) according to the manufacturer's instructions. Blood urea nitrogen (BUN) analysis was performed using a kit from BioAssay Systems (Hayward, CA).

Histology, IHC Staining, and Oil Red O Staining

Mice were perfused under anesthesia with PBS to remove blood from internal organs, including the liver. Perfused liver tissues were fixed in 4% paraformaldehyde for 4 hours at 4°C, rinsed with PBS, and dehydrated through ethanol and toluene. Dehydrated liver tissues were embedded in paraffin, and sections were cut at 5-μm thickness. Vascular structures were visualized by IHC staining with rat anti-CD31 (MEC 13.3; BD Biosciences, San Jose, CA) in conjunction with goat anti-rat IgG—horseradish peroxidase (Jackson ImmunoResearch Laboratories, West Grove, PA) and an Elite ABC kit (Vector Laboratories, Burlingame, CA). To detect liver lipid droplets, cryosections were prepared from fixed liver tissues, and stained with Oil Red O (Sigma-Aldrich, St. Louis, MO). Vascular lumen size and percentage areas occupied by vascular structures and lipid droplets were determined using the Adobe Photoshop CS4 Lasso tool, according to a procedure originally developed for quantifying neovascular tufts in the mouse OIR model.[36]

qPCR

Quantitative real-time PCR (qPCR) analyses were performed on an ABI PRISM 7900HT sequence detection system (Life Technologies, Carlsbad, CA) using SYBR Green PCR master mix (Life Technologies). The qPCR primers are listed in Table 1.

Table 1 qPCR Primer Sequences

Template	Forward	Reverse
Phd1	5′-CATCAATGGGCGCACCA-3′	5′-GATTGTCAACATGCCTCACGTAC-3′
Phd2	5′-TAAACGGCCGAACGAAAGC-3′	5′-GGGTTATCAACGTGACGGAC-3′
Phd3	5′-CTATGTCAAGGAGCGGTCCAA-3′	5′-GTCCACATGGCGAACATAACC-3′
VEGF-A	5′-CACGACAGAAGGAGAGCAGAAGT-3′	5′-TTCGCTGGTAGACATCCATGAA-3′
SDF1	5′-TCCTCTTGCTGTCCAGCTCT-3′	5′-CAGGCTGACTGGTTTACCG-3′
EPO	5′-TAGCCTCACTTCACTGCTTCG-3′	5′-GCTTGCAGAAAGTATCCACTGT-3′
FGF1	5′-GGACACCGAAGGGCTTTTAT-3′	5′-GCATGCTTCTTGGAGGTGTAA-3′
Ang1	5′-CGTCGTGTTCTGGAAGAATGA-3′	5′-CGTCGTGTTCTGGAAGAATGA-3′
Ang2	5′-CACACTGACCTTCCCCAACT-3′	5′-CCCACGTCCATGTCACAGTA-3′
FGF2	5′-CCAACCGGTACCTTGCTATG-3′	5′-GATTCCAGTCGTTCAAAGAAGAA-3′
MMP9	5′-CCTGAAAACCTCCAACCTCA-3′	5′-GGTGTAACCATAGCGGTACAAGT-3′

Western Blotting

Liver nuclear extracts were used for Western blotting. To prepare nuclear protein extracts, liver tissues were homogenized in ice-cold nuclear extraction buffer containing 10 mmol/L HEPES-KOH (pH 7.9), 1.5 mmol/L $MgCl_2$, 10 mmol/L KCl, 0.5 mmol/L dithiothreitol, 0.2 mmol/L phenylmethylsulfonyl fluoride, 0.2 mmol/L deferoxamine (Sigma-Aldrich), 0.1% NP-40, and 1× complete protease inhibitor cocktail (Roche Diagnostics, Indianapolis, IN). Nuclei were collected from homogenates by centrifugation. Pellets were resuspended in ice-cold buffer containing 20 mmol/L HEPES-KOH (pH 7.9), 420 mmol/L NaCl, 1.5 mmol/L $MgCl_2$, 0.5 mmol/L dithiothreitol, 0.2 mmol/L deferoxamine, 1× protease inhibitor cocktail, 0.2 mmol/L phenylmethylsulfonyl fluoride, and 25% glycerol. For Western blotting, the following antibodies were used: anti−HIF-1α (NB100-449; Novus Biologicals, Littleton, CO), anti−HIF-2α (NB100-122 and NB100-132; Novus Biologicals), and anti−β-actin (sc-1616; Santa Cruz Biotechnology, Dallas, TX). Band intensities were quantified using ImageJ 1.60 software (NIH, Bethesda, MD).

Erythroid EPO Sensitivity Assay

EPO sensitivity of erythroid cells was evaluated by a burst-forming unit−erythroid (BFU-E) colony formation assay in a methylcellulose-based semisolid culture medium (MethoCult M3234; STEMCELL Technologies, Vancouver, BC, Canada), supplemented with 20 ng/mL IL-3, 50 ng/mL stem cell factor (SCF) (PeproTech, Rocky Hill, NJ), and recombinant human EPO (rhEPO) in a range from 0 to 3000 mIU/mL (eBiosciences, San Diego, CA). Specifically, bone marrow cells were isolated from femurs, and plated out at 1×10^5 cells per dish (35 mm, low adhesion). BFU-E colonies were scored at 8 to 10 days after culturing at 37°C under 5% CO_2.

Labeling, Imaging, and Quantification of Retinal Blood Vessels

Eyes were enucleated from euthanized neonatal mice and were fixed in 4% paraformaldehyde for 40 minutes at room temperature. Retinas were dissected, flat-mounted with four incomplete radial incisions, and then stained with isolectin B_4 conjugated to Alexa Fluor 594 (Life Technologies). Stained retinas were analyzed by confocal imaging with a Zeiss LSM 510 Meta confocal microscope (Carl Zeiss Microscopy, Jena, Germany). Percentage areas of vascular obliteration and neovascularization were quantified using the Adobe Photoshop CS4 Lasso tool as described previously.[36]

Statistical Analysis

Statistical analyses were performed with two-tailed Student's *t*-test or two-way analysis of variance. Data are expressed as means ± SD or means ± SEM. All n values refer to the number of mice per group. $P < 0.05$ was considered significant.

Results

Changes in Hct Levels and EPO Expression Due to Hepatic Triple PHD Deficiency

To achieve hepatocyte-specific *Phd* disruption, we crossed mice carrying floxed *Phd1, Phd2, and Phd3* with Alb^{Cre} transgenic mice,[33] generating mice with a variety of floxed *Phd* loci and the Alb^{Cre} transgene. In $Phd1^{f/f}/Phd2^{f/f}/Phd3^{f/f}/Alb^{Cre}$ (*Phd(1/2/3)*hKO) mice, Phd1, Phd2, and Phd3 mRNA levels were reduced by approximately 70%, as estimated by qPCR of total liver RNA (Supplemental Figure S1A). Given that the liver also contains other cell types, such as endothelial cells, the specific percentage losses in hepatocytes were likely higher. As expected, HIF-1α and HIF-2α protein levels were increased in liver nuclear extracts from *Phd(1/2/3)*hKO mice (Supplemental Figure S1, B and C). qPCR analyses of total liver RNA demonstrated increased expression of VEGF-A, EPO, angiopoietin 2 (Ang2), and FGF2 species in *Phd(1/2/3)*hKO mice (Supplemental Figure S1D).

At 6 weeks of age, *Phd(1/2/3)*hKO mice had Hct values of 82.4 ± 7.2% (Figure 1A) and substantially increased blood Hb levels (Figure 1B). Similarly, $Phd1^{f/f}/Phd2^{f/f}/Phd3^{f/+}/Alb^{Cre}$ ($Phd(1/2)^{f/f}/3^{f/+}$/hKO) and $Phd1^{f/+}/Phd2^{f/f}/Phd3^{f/f}/Alb^{Cre}$ ($Phd1^{f/+}$/(2/3)hKO) mice both had significantly

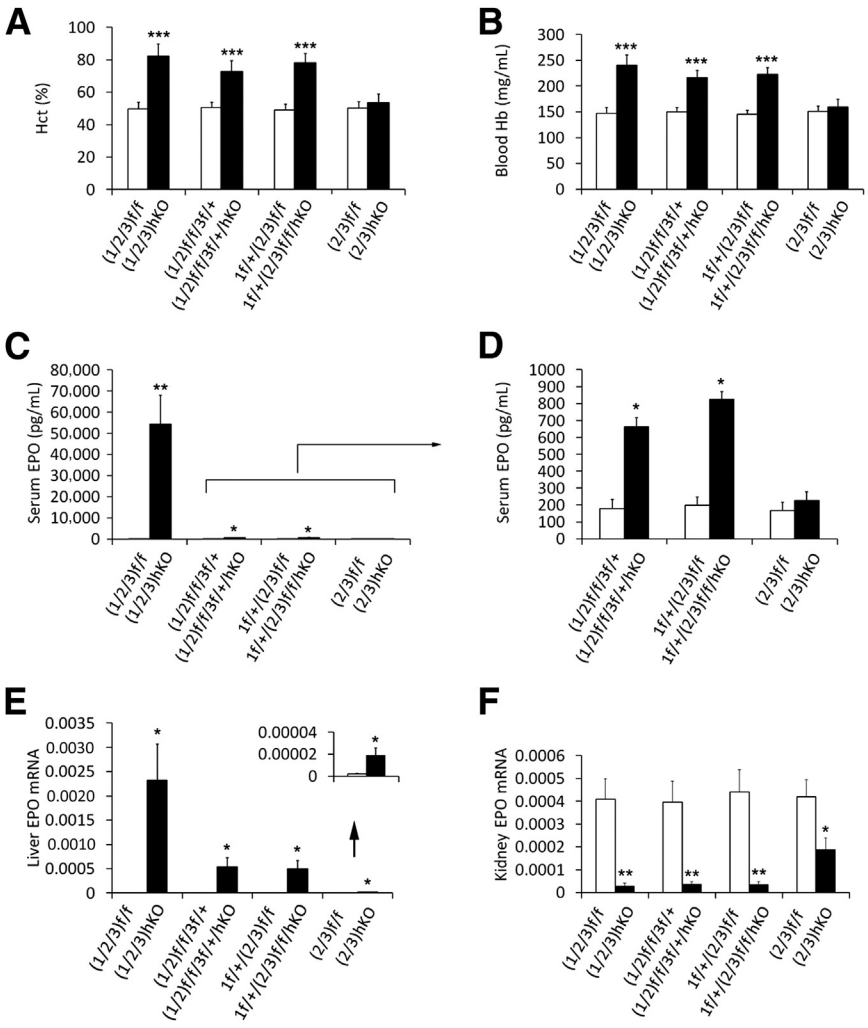

Figure 1 Effects of hepatic PHD deficiency on blood phenotypes and EPO expression. **A:** Hct values. **B:** Blood Hb concentrations. **C** and **D:** Serum EPO levels determined by ELISA. The scale in **D** allows resolution of EPO levels too low for the scale in **C** (**bracket** and **arrow**). **E** and **F:** EPO mRNA abundance, expressed as EPO/β-actin qPCR signal ratios. Values too low for the main scale (**arrow**) are presented at higher resolution in the **inset** (**E**). Data are expressed as means ± SD (**A** and **B**) or means ± SEM (**C**—**F**). $n = 5$ to 8 (**A** and **B**) or $n = 6$ to 8 (**C**—**F**). $^{*}P < 0.05$, $^{**}P < 0.01$, and $^{***}P < 0.001$, Student's *t*-test.

elevated Hct and Hb values (Figure 1, A and B). Consistent with these changes, serum EPO concentrations were increased in mice of all three groups (Figure 1, C and D), but EPO increases in *Phd(1/2/3)*hKO mice were by far the most dramatic, with an average of 135-fold increase over floxed controls (Figure 1C).

Increased serum EPO levels were due exclusively to liver EPO up-regulation. For example, hepatic EPO qPCR signals were increased 1246-fold in *Phd(1/2/3)*hKO mice and 338-fold in $Phd1^{f/+}$*/(2/3)*hKO mice (Figure 1E). Elevated liver EPO expression was accompanied by reduced EPO expression in kidney. In *Phd(1/2/3)*hKO mice, renal EPO expression was reduced to 6.7% of normal levels, and expression in $Phd(1/2)^{f/f}/3^{f/+}$/hKO and $Phd1^{f/+}$*/(2/3)*hKO mice was also dramatically reduced (Figure 1F).

In addition to comparisons between PHD-deficient mice and the respective floxed mice, we made additional comparisons across the various PHD-deficient mice (Supplemental Figure S2, A and B). The *Phd(1/2/3)*hKO mice had significantly higher serum EPO than either $Phd\ (1/2)^{f/f}/3^{f/+}$/hKO or $Phd1^{f/+}$*/(2/3)*hKO mice, although differences in Hct levels were not statistically significant. These findings suggest that further EPO increases beyond those observed in $Phd(1/2)^{f/f}/3^{f/+}$/hKO and $Phd1^{f/+}$*/(2/3)*hKO mice had little effect, presumably because at such high levels EPO availability is no longer a limiting factor.

Because polycythemia associated with pVHL deficiency or HIF-2α stabilization induces EPO hypersensitivity in erythroid cells,[37–39] we tested whether erythroid cells in $Phd1^{f/+}$*/(2/3)*hKO mice are also more sensitive to EPO. In brief, bone marrow cells were isolated from femurs and were cultured in semisolid MethoCult medium (STEMCELL Technologies) supplemented with appropriate cytokines and different amounts of rhEPO. Our data indicate that erythroid cells from $Phd1^{f/+}$*/(2/3)*hKO and floxed mice responded similarly to stimulation by different concentrations of recombinant EPO (Supplemental Figure S3), probably because PHD disruption in these mice was limited to hepatocytes but did not perturb the oxygen-sensing mechanism in erythroid cells. In experiments in which EPO hypersensitivity was observed, pVHL deficiency or HIF-2α stabilization was global, and EPO receptor expression was elevated in erythroid cells because of HIF-2α stabilization in these cells.

Vascular and Lipid Phenotypes in Triple—PHD-Deficient Livers

Because *Vhl* knockout led to vascular tumor formation and fatty liver phenotypes,[23] we wondered whether hepatic PHD deficiency might have similar effects. We examined vascular morphology by anti-CD31 IHC staining of liver sections (Figure 2, A—H) and quantified the findings (Figure 2, Q and R). Vascular lumen sizes were increased 410% in *Phd(1/2/3)*hKO mice and 52% in $Phd1^{f/+}$*/(2/3)* hKO mice, but insignificantly in $Phd(1/2)^{f/f}/3^{f/+}$/hKO mice. The differences between *Phd(1/2/3)*hKO and other mice were significant (Supplemental Figure S2C). Percentage area occupied by vascular structures was increased in all *Phd(1/2/3)*hKO, $Phd(1/2)^{f/f}/3^{f/+}$/hKO, and $Phd1^{f/+}$*/(2/3)* hKO mice, relative to their respective floxed controls. In contrast to pVHL-deficient mice, vascular tumors were not found in these PHD-deficient mice.

Oil Red O staining indicated that liver lipid contents were increased in the aforementioned PHD-deficient mice (Figure 2, I—P). Quantification of percentage area occupied by lipid droplets showed a relative value of 11:1 between *Phd(1/2/3)* hKO and $Phd(1/2/3)^{f/f}$ mice, whereas $Phd(1/2)^{f/f}/3^{f/+}$/hKO and $Phd1^{f/+}$*/(2/3)*hKO mice displayed milder lipid accumulation (Supplemental Figure S2). Differential lipid accumulation between *Phd(1/2/3)*hKO mice and the other two lines was statistically significant (Supplemental Figure S2D).

*Phd(1/2/3)*hKO mice generally died by 8 weeks of age. Although the exact causes are unknown, it is conceivable that severe liver defects may have contributed to premature death. Although polycythemia is most likely harmful as well, it should be noted that both $Phd(1/2)^{f/f}/3^{f/+}$/hKO and $Phd1^{f/+}$*/(2/3)*hKO mice lived over a year, despite high Hct.

Resistance of $Phd(1/2)^{f/f}/Phd3^{f/+}$/hKO and $Phd1^{f/+}$*/(2/3)*hKO Mice to Renal Failure Anemia

Elevated liver EPO expression due to PHD deficiency might enable these mice to resist renal failure anemia. To address this possibility, we used a previously established procedure to induce chronic renal failure by adenine-rich diet.[29—32] In a pilot experiment with wild-type mice, adenine diet led to rapid and progressive increase in BUN concentrations over an 8-week period, whereas Hct values gradually decreased to severely anemic levels (31.3 ± 2.2%, means ± SEM) (data not shown). These findings confirmed that the adenine-diet model worked similarly in our hands as described in previous publications.[29—31]

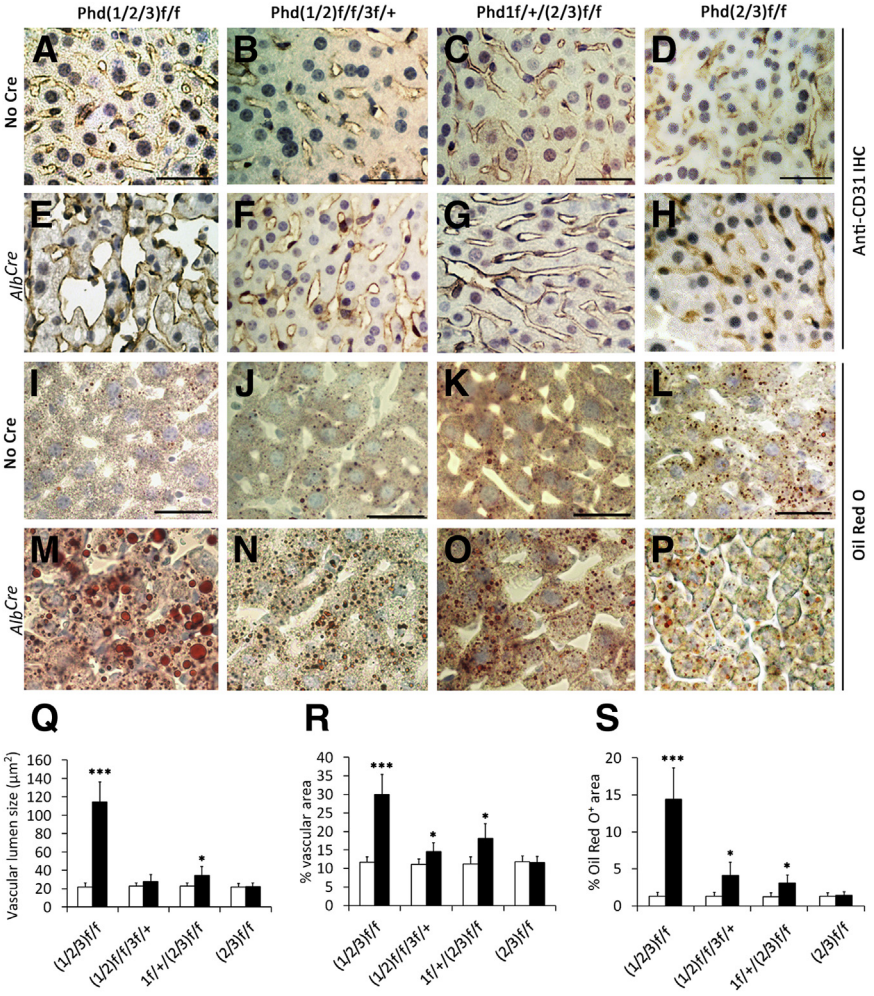

Figure 2 Liver vascular and lipid phenotypes associated with hepatic PHD deficiency. **A—H:** Anti-CD31 IHC staining of liver sections from adult mice differing in genotype (*Phd* loci) and in Alb^{Cre} transgene status. **I—P:** Oil Red O—stained liver sections. **Q—S:** Quantification of vascular lumen size (**Q**), percent area occupied by vascular structures (**R**), and percent area occupied by Oil Red O—positive lipid droplets (**S**). Mice were 6 weeks of age when analyzed. Data are expressed as means ± SD. $n = 5$ to 8. $^{*}P < 0.05$, $^{***}P < 0.001$, Student's *t*-test. Scale bar = 25 μm. Black bars, with Alb^{Cre}; white bars, no Alb^{Cre}.

When *Phd(1/2)*$^{f/f}$/*3*$^{f/+}$/hKO and *Phd1*$^{f/+}$/*(2/3)*hKO mice were switched to adenine-rich diet for 8 weeks between 8 and 16 weeks of age, BUN concentrations were significantly increased, as in floxed controls (Supplemental Figure S4, A and B). However, high Hct levels persisted, whereas all floxed controls developed severe anemia (Figure 3, A and B). Elevated Hct levels in the knockout mice were supported by several hundred-fold increases in liver EPO expression, both on normal chow and adenine-rich diet (Figure 3C). On normal chow, *Phd(1/2)*$^{f/f}$/*3*$^{f/+}$/hKO and *Phd1*$^{f/+}$/*(2/3)*hKO mice had reduced renal EPO expression, compared with floxed controls, whereas the adenine diet significantly reduced renal EPO expression in both *Phd(1/2)*$^{f/f}$/*3*$^{f/+}$ and *Phd1*$^{f/+}$/*(2/3)* mice (Figure 3D).

Normal Hematological and Liver Phenotypes in *Phd(2/3)*hKO Mice

In contrast to triple PHD deficiency, *Phd2*$^{f/f}$/*Phd3*$^{f/f}$/*Alb*^{Cre} (*Phd(2/3)*hKO) mice had an average Hct level of 53.5 ± 5.4%, which was not statistically different from the floxed controls (Figure 1A). Hb and serum EPO levels also were unaltered (Figure 1, B–D). Nonetheless, hepatic EPO expression was increased to 9.1-fold of normal baseline, whereas renal EPO expression was decreased to 45% of normal values (Figure 1, E and F). Besides the normal Hct and Hb levels, *Phd(2/3)*hKO mice were also apparently normal in liver vascular morphology and lipid contents (Figure 2, D, H, L, P, and Q–S). Life span was similar for *Phd(2/3)*hKO and wild-type mice.

On the adenine-rich diet, both *Phd(2/3)*$^{f/f}$ and *Phd(2/3)*hKO mice displayed increased BUN concentration (Supplemental Figure S4, C and D), as expected for compromised renal function. At the end of the 8-week period on the adenine diet, Hct levels remained normal in *Phd(2/3)*hKO mice (48.1 ± 1.8%), but decreased to 30.5 ± 2.0% in *Phd(2/3)*$^{f/f}$ mice (Figure 4A). In both groups of mice, there was no apparent vascular malformation or liver steatosis after adenine treatment (Supplemental Figure S5). Thus, hepatic PHD2 and PHD3 double deficiency protected mice from adenine-induced anemia without inflicting other abnormalities such as erythrocytosis, vascular malformation, and liver steatosis.

Serum EPO ELISA did not reveal statistically significant differences between *Phd(2/3)*hKO and *Phd(2/3)*$^{f/f}$ mice, nor between mice on normal chow versus the adenine diet (Figure 4B). At least in the case of *Phd(2/3)*$^{f/f}$ mice, our failure to detect reduced serum EPO after adenine treatment could have been due to sensitivity and/or accuracy issues below basal level concentrations, because adenine-treated *Phd(2/3)*$^{f/f}$ mice exhibited all other signs consistent with reduced serum EPO, including severe anemia, lack of significant EPO up-regulation in the liver, and severely reduced renal EPO mRNA levels.

Because *Phd(2/3)*hKO mice resisted adenine-induced anemia, we asked whether hepatic deficiency of a single PHD isoform might confer similar Hct stability. On normal chow, *Phd1*$^{f/f}$/*Alb*^{Cre}, *Phd2*$^{f/f}$/*Alb*^{Cre}, and *Phd3*$^{f/f}$/*Alb*^{Cre} mice all had normal Hct levels; when fed with the adenine diet for 8 weeks, all of these mice developed severe anemia (Supplemental Figure S6). These data indicate that targeting a single PHD isoform in the liver is not sufficient to resist renal failure-induced anemia.

Sensitized Liver EPO Induction by Systemic Hypoxia in *Phd(2/3)*hKO Mice

Once switched to the adenine diet, *Phd(2/3)*hKO mice maintained normal Hct levels by further up-regulating liver

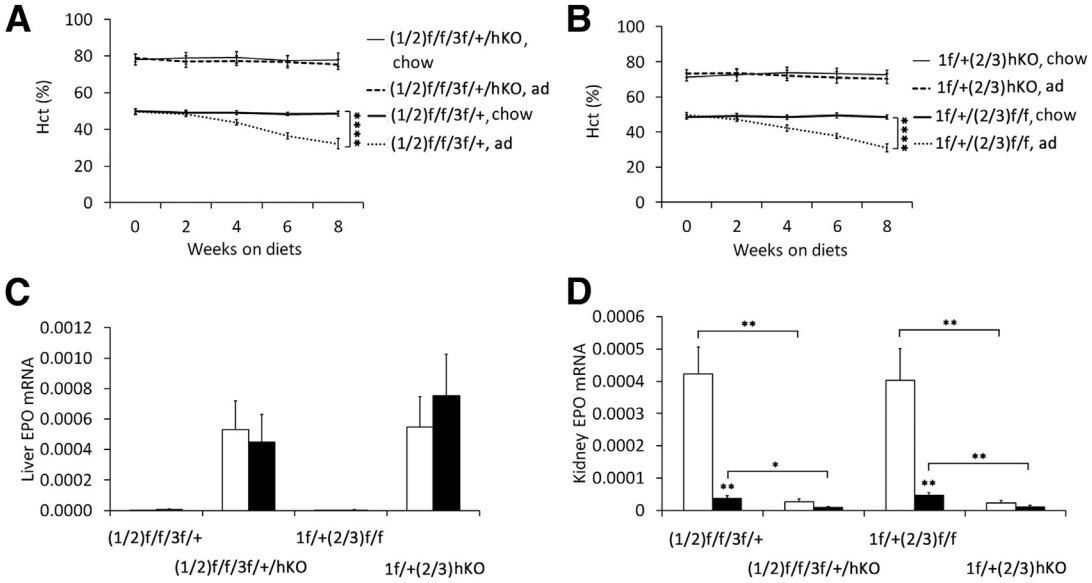

Figure 3 Resistance of *Phd1*$^{f/+}$/*(2/3)*hKO and *Phd(1/2)*$^{f/f}$/*3*$^{f/+}$/hKO mice to adenine-induced chronic anemia. **A** and **B:** Hct in *Phd(1/2)*$^{f/f}$/*3*$^{f/+}$/hKO (**A**) and *Phd1*$^{f/+}$/*(2/3)*hKO (**B**) mice on normal chow or an adenine-rich diet. Baseline blood samples at week 0 were taken just before diet switching. **C** and **D:** qPCR analyses for liver (**C**) and kidney (**D**) EPO expression, relative to β-actin. Data are expressed as means ± SEM. $n = 6$. $^*P < 0.05$, $^{**}P < 0.01$, and $^{****}P < 0.0001$, two-way analysis of variance (**A** and **B**) or Student's *t*-test (**C** and **D**). Black bars, adenine; white bars, chow. ad, adenine diet; chow, normal chow diet.

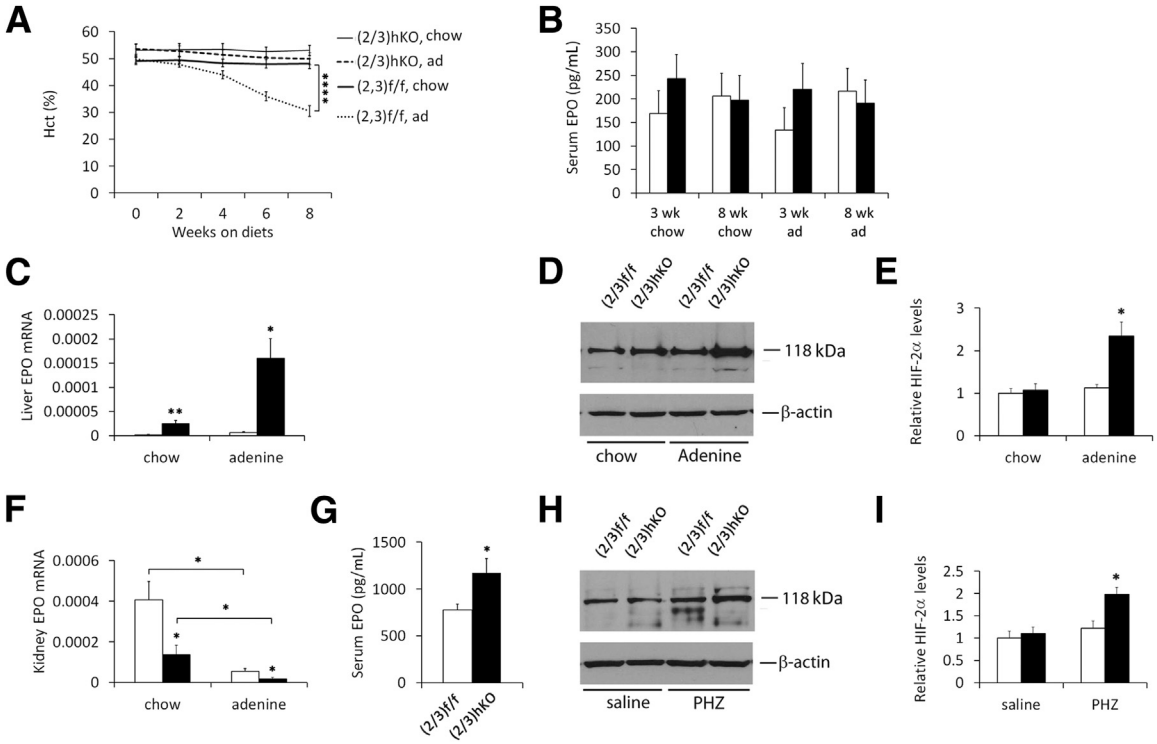

Figure 4 Maintenance of normal blood homeostasis in *Phd(2/3)*hKO mice by sensitized liver EPO induction. **A:** Hct values for *Phd(2/3)*hKO and *Phd(2/3)*$^{f/f}$ mice. All mice were initially maintained on normal chow until 8 weeks of age, after which they were either continued on normal chow or switched to an adenine-rich diet. Baseline blood samples at week 0 were taken just before diet switching. **B:** Serum EPO quantification by ELISA at 3 weeks and 8 weeks after diet switching. **C:** qPCR analysis of liver EPO mRNA levels, normalized to β-actin. **D:** Representative anti—HIF-2α Western blots of liver nuclear extracts from mice on normal chow or 3 weeks on an adenine diet. The HIF-2α band is detected at approximately 118 kDa. **E:** Corresponding quantification of HIF-2α bands. **F:** Kidney EPO mRNA levels, normalized to β-actin. **G:** Serum EPO levels in 8-week-old mice injected with PHZ at 40 mg/kg. Two doses of PHZ were injected 24 hours apart, and mice were euthanized for analysis at 48 hours after the second injection. **H:** Representative anti—HIF-2α Western blots of liver nuclear extracts from PHZ- or saline-injected mice. HIF-2α was detected at 118 kDa. **I:** Corresponding quantification of HIF-2α bands. Data are expressed as means ± SEM. $n = 6$ (**A** and **B**); $n = 5$ (**C** and **F**); $n = 3$ (**D**, **E**, **H**, and **I**). $^{*}P < 0.05$, $^{**}P < 0.01$, and $^{****}P < 0.0001$, two-way analysis of variance (**A**) or Student's *t*-test (**B**—**E**, **G**, and **H**). Black bars, *PhD(2/3)*hKO; white bars, *PhD(2/3)*$^{f/f}$.

EPO expression over their already up-regulated levels on normal chow. Similar increases were not observed in adenine-treated *Phd(2/3)*$^{f/f}$ mice (Figure 4C). At the protein level, adenine-treated *Phd(2/3)*hKO mice accumulated higher HIF-2α levels in the liver (Figure 4, D and E), consistent with sensitized response to systemic hypoxia. In the kidney, EPO mRNA levels were reduced substantially in adenine-treated mice, both in *Phd(2/3)*hKO and *Phd(2/3)*$^{f/f}$ groups (Figure 4F). On both normal chow and the adenine diet, *Phd(2/3)*hKO mice displayed lower renal EPO expression levels than *Phd(2/3)*$^{f/f}$ controls.

To complement the adenine diet experiment, we induced acute hemolysis by phenylhydrazine (PHZ). At 2 days after PHZ injection at the 40 mg/kg dose, serum EPO concentrations in *Phd(2/3)*hKO mice were 50.4% higher than in similarly treated floxed mice (Figure 4G). In addition, HIF-2α accumulation selectively occurred in PHZ-treated *Phd(2/3)*hKO mice (Figure 4, H and I).

To further investigate sensitivity to systemic hypoxia, we tested the effects of different PHZ doses. As expected, higher PHZ doses induced more severe anemia in both *Phd(2/3)*hKO and *Phd(2/3)*$^{f/f}$ mice (Figure 5A). Lack of compensatory Hct up-regulation in *Phd(2/3)*hKO mice can be explained by the acute nature of the experiment. Serum EPO concentration increased more substantially with larger doses of PHZ injection (Figure 5B), apparently as a feedback response to more severe hemolytic anemia. Importantly, *Phd(2/3)*hKO mice had higher serum EPO levels than floxed controls at the 40 mg/kg and 80 mg/kg doses, indicating that these mice were able to respond to anemia (hypoxia) more sensitively. In support of this possibility, liver EPO induction in *Phd(2/3)*hKO mice had more sensitive dose responses (Figure 5, C and D). In kidney, PHZ-dependent anemia also triggered EPO up-regulation, but without noticeable differences between *Phd(2/3)*hKO and *Phd(2/3)*$^{f/f}$ mice (Figure 5, E and F). Overall, these data suggest that *Phd(2/3)*hKO mice were sensitized for hepatic EPO induction in response to systemic hypoxia.

Oxygen-Induced Obliteration of Retinal Microvessels in Neonatal Mice Triple Deficient for Hepatic PHDs

Retinopathy of prematurity, a leading cause of blindness in children, is typically associated with oxygen therapy for

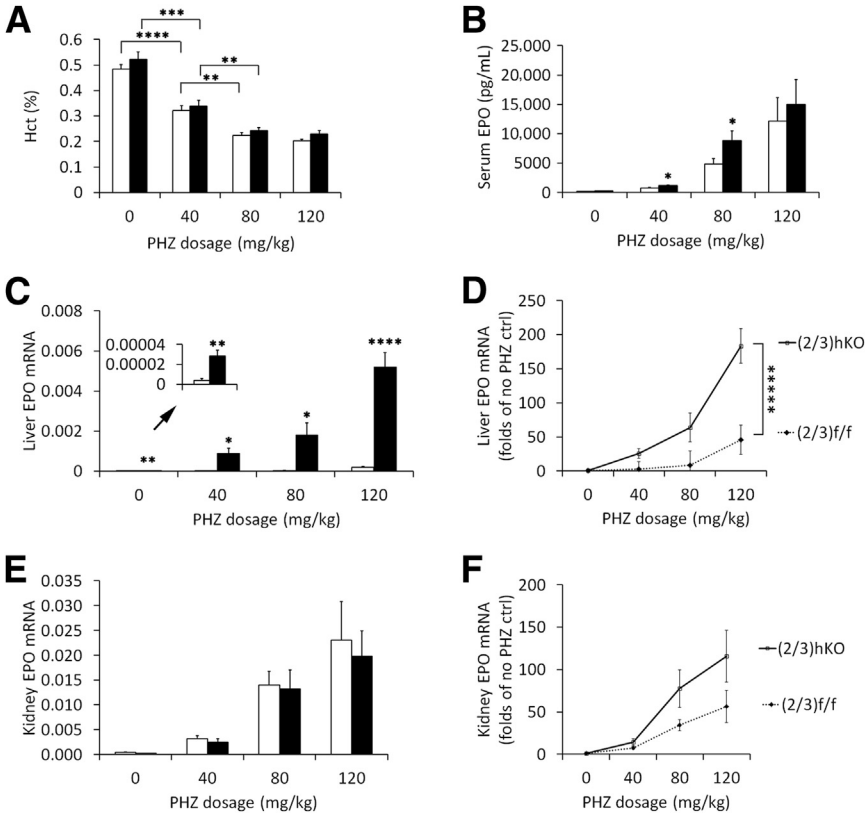

Figure 5 PHZ dose response in *Phd(2/3)*$^{f/f}$ and *Phd(2/3)*hKO mice. Two doses of PHZ were injected 24 hours apart, and mice were euthanized at 48 hours after the second injection. **A:** Hct values at 0, 40, 80, and 120 mg/kg/dose. **B:** Serum EPO protein levels determined by ELISA. **C:** Liver EPO qPCR analysis, normalized to β-actin. Values too low for the main scale (**arrow**) are presented at higher resolution in the **inset**. **D:** Dose response of liver EPO mRNA induction, presented as fold change of EPO mRNA abundance relative to that in saline-injected, genotype-matched control mice. PHD dose response was more sensitive in *Phd(2/3)* hKO mice. **E:** Kidney EPO qPCR signals normalized against β-actin. **F:** Dose response of kidney EPO mRNA induction (fold change relative to baseline values in saline-injected, genotype-matched control mice). Data are expressed as means ± SEM. $n = 6$ (**A** and **D**); $n = 6$ to 11 (**B**, **C**, **E**, and **F**). $^{*}P < 0.05$, $^{**}P < 0.01$, $^{***}P < 0.001$, $^{****}P < 0.0001$, and $^{*****}P < 0.00001$, Student's *t*-test (**A**–**C**, and **E**) and two-way analysis of variance (**D**) for interaction between PHZ dose and EPO mRNA abundance. $P = 0.16$, two-way analysis of variance for interaction (**F**). Black bars, *(2/3)*hKO; white bars, *(2/3)*$^{f/f}$.

premature infants. In mice, retinopathy of prematurity–like phenotypes can be mimicked by OIR. In the OIR model, neonatal mice are exposed to 75% oxygen for 5 days between postnatal days P7 and P12 (phase I) followed by another 5 days (P12 to P17) in ambient room air (phase II).[34,35] In phase I, significant microvascular obliteration occurs. Upon return to ambient air, poor perfusion due to vascular loss leads to severe hypoxia and neovascularization. EPO appears to play a protective role in these processes, because delivery of exogenous EPO to mice protects retinal microvessels in phase I and reduces neovascularization in phase II.[40] In a related study, systemic delivery of a PHD inhibitor (dimethyloxalylglycine) to neonatal mice promoted EPO expression and protected retinal microvessels from hyperoxia-induced damages.[41] Interestingly, there were indications that inhibition of hepatic PHDs might be responsible for the protection of retinal vasculature.

To determine whether triple PHD deficiency in the liver might have similar effects on the retina, we exposed *Phd(1/2/3)*hKO and *Phd(1/2/3)*$^{f/f}$ mice to 75% oxygen from P7 to P12 and analyzed retinal vasculature at P12 immediately after oxygen treatment or at P17 after 5 days in ambient air. At P12, *Phd(1/2/3)*hKO and *Phd(1/2/3)*$^{f/f}$ mice exhibited similar levels of microvascular obliteration (Figure 6, A–C). At P17, robust neovascularization was present to a similar extent in both groups of mice (Figure 6, D–G). These data indicate that hepatic deficiency of all three PHD isoforms failed to protect retinas from oxygen-induced vascular injury.

Discussion

Differential Blood and Liver Phenotypes among Various Hepatic PHD-Deficient Mice

Several studies have demonstrated elevated EPO expression and erythropoiesis in PHD-deficient mice.[8,9,27] In particular, a recent study in an acute renal injury model demonstrated the feasibility of treating anemia by targeting hepatic PHDs.[28] Nonetheless, several important issues remain to be addressed. First, although the ability to promote EPO expression and erythropoiesis offers new opportunities for treating anemia, the associated polycythemia is a health concern. Second, because hepatic pVHL deficiency led to vascular tumors and fatty liver phenotype,[23] it is important to determine whether PHD-deficient livers develop similar phenotypes. Third, it remains to be determined whether hepatic PHDs are effective targets for treating anemia in a chronic kidney disease model.

To better understand the roles of liver PHDs, we compared how hepatic disruption of different combinations of PHD isoforms might affect blood, vascular, and lipid phenotypes. Although deficiency of all three PHD isoforms in *Phd(1/2/3)* hKO mice caused severe erythrocytosis, as well as extensive vascular malformation and massive accumulation of lipid droplets in the liver, the presence of a single wild-type *Phd1* or *Phd3* allele in *Phd1*$^{f/+}$*/(2/3)*hKO or *Phd(1/2)*$^{f/f}$*/3*$^{f/+}$/hKO mice minimized hepatic vascular and lipid abnormalities, although severe erythrocytosis persisted. In mice double-deficient for

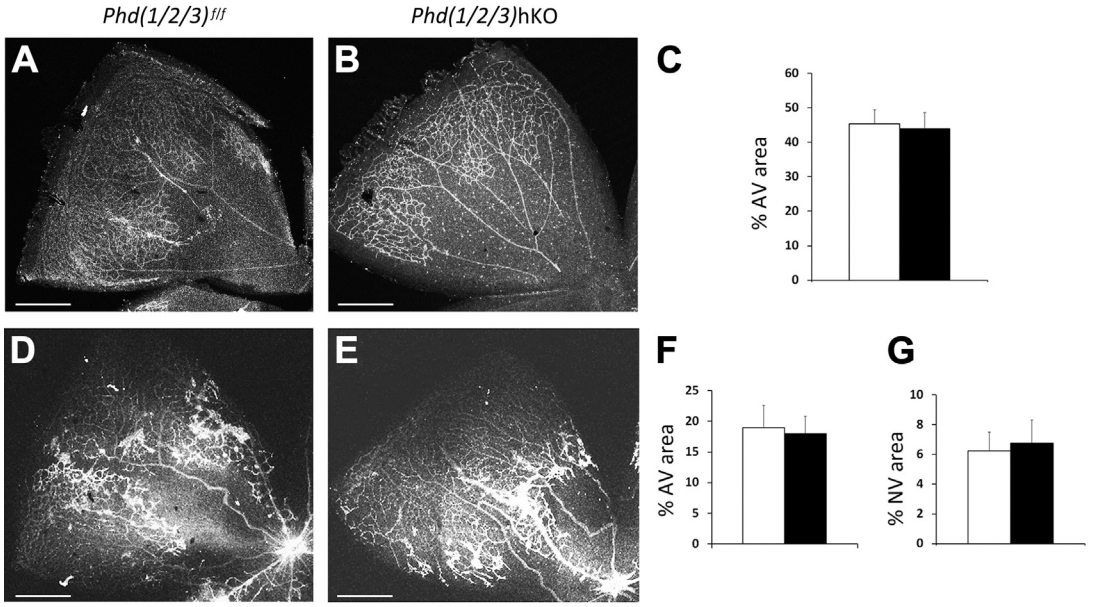

Figure 6 Analysis of *Phd(1/2/3)*hKO mice by OIR model. **A** and **B**: Neonatal *Phd(1/2/3)*hKO mice (**B**) and their floxed controls (**A**) were exposed to 75% oxygen for 5 days between P7 and P12; the mice were euthanized immediately after oxygen treatment, to examine the extent of vascular obliteration. Retinas were fixed in 4% paraformaldehyde, flat-mounted with four incomplete radial incisions, and then stained with isolectin B_4 conjugated to Alexa Fluor 594. Confocal images of representative petals are shown. **C:** Vascular obliteration is shown as percent avascular areas. **D** and **E:** Neovascularization in *Phd(1/2/3)* hKO mice (**E**) and their floxed controls (**D**) after OIR phase II. Retinas were dissected from P17 mice after 5 days of oxygen exposure (P7 to P12) and another 5 days in ambient air (P12 to P17) and then were stained with isolectin B_4—Alexa Fluor 594. Confocal images of representative petals are shown. **F** and **G:** Percent area that remained avascular (**F**) and percent area occupied by neovascular tufts (**G**). Data are expressed as means ± SEM. $n = 6$ (**C**); $n = 4$ (**F** and **G**). Scale bars: 500 μm. Black bars, *Phd(1/2/3)*hKO; white bars, *Phd(1/2/3)*$^{f/f}$. AV, avascular; NV, neovascular tufts.

hepatic PHD2 and PHD3, Hct levels remained within a healthy range on either normal chow or the kidney-damaging adenine diet, and vascular morphology and lipid deposition appeared normal in the liver. These observations demonstrate that liver vascular and lipid defects can be minimized or avoided by targeting selective combinations of hepatic PHD isoforms. Meanwhile, we note that our data do not exclude other isoform combinations as valid targets, such as limited knockdown of all three PHD isoforms.

EPO Regulation in Mice Deficient for Hepatic PHDs

Phd1$^{f/+}$*/(2/3)*hKO mice exhibited several hundredfold increases in liver EPO mRNA, but only severalfold increases in serum EPO protein. This apparent paradox can be better understood by considering at least two issues. First, kidney EPO expression is dramatically reduced in these mice, presumably because of feedback inhibition by vastly up-regulated liver EPO production. Second, because of very low baseline levels of EPO in normal livers, each fold increase in liver EPO mRNA corresponds to only a small fraction of the EPO expression capacity in normal kidney. Based on basal EPO mRNA levels in the liver and kidney, and at an approximate mass ratio of 4:1 between the liver and two kidneys, the amount of EPO mRNA in a *Phd1*$^{f/+}$*/(2/3)*hKO liver roughly corresponds to the combined amounts from seven pairs of normal kidneys.

Although these estimates are unlikely to be completely accurate because of several inherently crude assumptions (eg, equal translational efficiencies in liver and kidney), they do help explain why serum EPO is increased by only severalfold (instead of fold changes in the tens and hundreds) in *Phd1*$^{f/+}$*/(2/3)*hKO mice. By a similar argument, it is not surprising that serum EPO in *Phd(2/3)*hKO mice was essentially unchanged, despite the approximately ninefold up-regulation in liver EPO expression. On the adenine diet, further up-regulated liver EPO expression might have been offset by compromised renal EPO expression.

Sensitized EPO Induction in PHD2 and PHD3 Double Deficient Livers

We examined whether PHD2 and PHD3 double-deficient liver is more sensitive to modest anemia (systemic hypoxia). After adenine treatment, elevated HIF-2α protein levels were detected in *Phd(2/3)*hKO but not *Phd(2/3)*$^{f/f}$ mice. Although *Phd(2/3)*hKO mice were never anemic on either normal chow or the adenine diet, increased HIF-2α protein accumulation on the adenine diet suggests that the liver in these mice was very sensitive to minor downward drifting in Hct levels and compensated for such changes by HIF-2α accumulation and hepatic EPO up-regulation, thus preventing further Hct reduction.

We also investigated EPO expression regulation by inducing hemolytic anemia with PHZ. After PHZ injection, *Phd(2/3)*$^{f/f}$ and *Phd(2/3)*hKO mice developed similar levels of anemia. The failure of *Phd(2/3)*hKO mice to maintain normal Hct levels was apparently due to the acute nature of

PHZ-induced hemolysis. Liver EPO expression was increased in both *Phd(2/3)*$^{f/f}$ and *Phd(2/3)*hKO mice, but much more robustly in the latter group. As an indication of more sensitive response to modest anemia in *Phd(2/3)*hKO mice, low-dose PHZ injection promoted liver HIF-2α protein accumulation more effectively in these mice.

Serum EPO levels were up-regulated with increasing PHZ doses. Because kidneys remained functional in these experiments, up-regulated renal EPO expression in response to anemia may account for most of the blood EPO increases in PHZ-treated floxed mice. On the other hand, additional serum EPO increases in *Phd(2/3)*hKO mice may be due to up-regulated liver EPO expression. As expected, the highest PHZ dose induced the highest serum EPO levels, but the distinction between *Phd(2/3)*hKO and floxed mice was not obvious at this dose. It is likely that robust renal EPO induction under this condition overshadowed differential liver EPO expression between *Phd(2/3)*hKO and *Phd(2/3)*$^{f/f}$ mice. Overall, our data indicate that hepatic PHD2 and PHD3 double deficiency indeed confers sensitized response to systemic hypoxia.

Liver EPO Expression and Oxygen-Induced Retinopathy

Because systemically elevated EPO levels as well as chemical inhibition of hepatic PHDs had been previously reported to protect retinal microvessels from oxygen-induced losses, we also examined *Phd(1/2/3)*hKO mice by the OIR model. Retinal microvessels were similarly obliterated by oxygen in *Phd(1/2/3)*hKO and *Phd(1/2/3)*$^{f/f}$ mice. At present, there are no simple explanations for the discrepancy between our findings and those in the literature, but several possibilities exist. For example, retinal vascular protection by recombinant EPO was found to be dose dependent.[40] It is possible that, at the responsive doses, recipient mice received even larger amounts of EPO than was produced in *Phd(1/2/3)*hKO mice. With regard to PHD inhibitor–mediated protection of retinal blood vessels, hepatic and retinal EPO expression were both elevated, and the latter might have made at least some contribution.[41] At any rate, consideration of our genetic data in conjunction with earlier findings should facilitate the optimization of EPO-based therapies for retinal protection.

Supplemental Data

Supplemental material for this article can be found at *http://dx.doi.org/10.1016/j.ajpath.2013.12.014*.

References

1. Epstein AC, Gleadle JM, McNeill LA, Hewitson KS, O'Rourke J, Mole DR, Mukherji M, Metzen E, Wilson MI, Dhanda A, Tian YM, Masson N, Hamilton DL, Jaakkola P, Barstead R, Hodgkin J, Maxwell PH, Pugh CW, Schofield CJ, Ratcliffe PJ: C. elegans EGL-9 and mammalian homologs define a family of dioxygenases that regulate HIF by prolyl hydroxylation. Cell 2001, 107:43–54
2. Bruick RK, McKnight SL: A conserved family of prolyl-4-hydroxylases that modify HIF. Science 2001, 294:1337–1340
3. Ivan M, Haberberger T, Gervasi DC, Michelson KS, Günzler V, Kondo K, Yang H, Sorokina I, Conaway RC, Conaway JW, Kaelin WG Jr: Biochemical purification and pharmacological inhibition of a mammalian prolyl hydroxylase acting on hypoxia-inducible factor. Proc Natl Acad Sci USA 2002, 99:13459–13464
4. Maxwell PH, Wiesener MS, Chang GW, Clifford SC, Vaux EC, Cockman ME, Wykoff CC, Pugh CW, Maher ER, Ratcliffe PJ: The tumour suppressor protein VHL targets hypoxia-inducible factors for oxygen-dependent proteolysis. Nature 1999, 399:271–275
5. Takeda K, Ho VC, Takeda H, Duan LJ, Nagy A, Fong GH: Placental but not heart defects are associated with elevated hypoxia-inducible factor alpha levels in mice lacking prolyl hydroxylase domain protein 2. Mol Cell Biol 2006, 26:8336–8346
6. Takeda K, Cowan A, Fong GH: Essential role for prolyl hydroxylase domain protein 2 in oxygen homeostasis of the adult vascular system. Circulation 2007, 116:774–781
7. Mazzone M, Dettori D, Leite de Oliveira R, Loges S, Schmidt T, Jonckx B, Tian YM, Lanahan AA, Pollard P, Ruiz de Almodovar C, De Smet F, Vinckier S, Aragonés J, Debackere K, Luttun A, Wyns S, Jordan B, Pisacane A, Gallez B, Lampugnani MG, Dejana E, Simons M, Ratcliffe P, Maxwell P, Carmeliet P: Heterozygous deficiency of PHD2 restores tumor oxygenation and inhibits metastasis via endothelial normalization. Cell 2009, 136:839–851
8. Takeda K, Aguila HL, Parikh NS, Li X, Lamothe K, Duan LJ, Takeda H, Lee FS, Fong GH: Regulation of adult erythropoiesis by prolyl hydroxylase domain proteins. Blood 2008, 111:3229–3235
9. Minamishima YA, Moslehi J, Bardeesy N, Cullen D, Bronson RT, Kaelin WG Jr: Somatic inactivation of the PHD2 prolyl hydroxylase causes polycythemia and congestive heart failure. Blood 2008, 111:3236–3244
10. Percy MJ, Furlow PW, Beer PA, Lappin TR, McMullin MF, Lee FS: A novel erythrocytosis-associated PHD2 mutation suggests the location of a HIF binding groove. Blood 2007, 110:2193–2196
11. Hölscher M, Silter M, Krull S, von Ahlen M, Hesse A, Schwartz P, Wielockx B, Breier G, Katschinski DM, Zieseniss A: Cardiomyocyte-specific prolyl-4-hydroxylase domain 2 knock out protects from acute myocardial ischemic injury. J Biol Chem 2011, 286:11185–11194
12. Moslehi J, Minamishima YA, Shi J, Neuberg D, Charytan DM, Padera RF, Signoretti S, Liao R, Kaelin WG Jr: Loss of hypoxia-inducible factor prolyl hydroxylase activity in cardiomyocytes phenocopies ischemic cardiomyopathy. Circulation 2010, 122:1004–1016
13. Hyvärinen J, Hassinen IE, Sormunen R, Mäki JM, Kivirikko KI, Koivunen P, Myllyharju J: Hearts of hypoxia-inducible factor prolyl 4-hydroxylase-2 hypomorphic mice show protection against acute ischemia-reperfusion injury. J Biol Chem 2010, 285:13646–13657
14. Ginouvès A, Ilc K, Macías N, Pouysségur J, Berra E: PHDs overactivation during chronic hypoxia "desensitizes" HIFalpha and protects cells from necrosis. Proc Natl Acad Sci USA 2008, 105:4745–4750
15. Aragonés J, Schneider M, Van Geyte K, Fraisl P, Dresselaers T, Mazzone M, et al: Deficiency or inhibition of oxygen sensor Phd1 induces hypoxia tolerance by reprogramming basal metabolism. Nat Genet 2008, 40:170–180
16. Rius J, Guma M, Schachtrup C, Akassoglou K, Zinkernagel AS, Nizet V, Johnson RS, Haddad GG, Karin M: NF-kappaB links innate immunity to the hypoxic response through transcriptional regulation of HIF-1alpha. Nature 2008, 453:807–811
17. Cummins EP, Berra E, Comerford KM, Ginouves A, Fitzgerald KT, Seeballuck F, Godson C, Nielsen JE, Moynagh P, Pouyssegur J, Taylor CT: Prolyl hydroxylase-1 negatively regulates IkappaB kinase-beta, giving insight into hypoxia-induced NFkappaB activity. Proc Natl Acad Sci USA 2006, 103:18154–18159
18. Takeda Y, Costa S, Delamarre E, Roncal C, Leite de Oliveira R, Squadrito ML, Finisguerra V, Deschoemaeker S, Bruyère F, Wenes M,

Hamm A, Serneels J, Magat J, Bhattacharyya T, Anisimov A, Jordan BF, Alitalo K, Maxwell P, Gallez B, Zhuang ZW, Saito Y, Simons M, De Palma M, Mazzone M: Macrophage skewing by Phd2 haplodeficiency prevents ischaemia by inducing arteriogenesis. Nature 2011, 479:122−126
19. Jelkmann W: Molecular biology of erythropoietin. Intern Med 2004, 43:649−659
20. Koivunen P, Tiainen P, Hyvärinen J, Williams KE, Sormunen R, Klaus SJ, Kivirikko KI, Myllyharju J: An endoplasmic reticulum transmembrane prolyl 4-hydroxylase is induced by hypoxia and acts on hypoxia-inducible factor alpha. J Biol Chem 2007, 282:30544−30552
21. Laitala A, Aro E, Walkinshaw G, Mäki JM, Rossi M, Heikkilä M, Savolainen ER, Arend M, Kivirikko KI, Koivunen P, Myllyharju J: Transmembrane prolyl 4-hydroxylase is a fourth prolyl 4-hydroxylase regulating EPO production and erythropoiesis. Blood 2012, 120: 3336−3344
22. Nangaku M: Chronic hypoxia and tubulointerstitial injury: a final common pathway to end-stage renal failure. J Am Soc Nephrol 2006, 17:17−25
23. Haase VH, Glickman JN, Socolovsky M, Jaenisch R: Vascular tumors in livers with targeted inactivation of the von Hippel-Lindau tumor suppressor. Proc Natl Acad Sci USA 2001, 98:1583−1588
24. Rankin EB, Biju MP, Liu Q, Unger TL, Rha J, Johnson RS, Simon MC, Keith B, Haase VH: Hypoxia-inducible factor-2 (HIF-2) regulates hepatic erythropoietin in vivo. J Clin Invest 2007, 117:1068−1077
25. Kapitsinou PP, Liu Q, Unger TL, Rha J, Davidoff O, Keith B, Epstein JA, Moores SL, Erickson-Miller CL, Haase VH: Hepatic HIF-2 regulates erythropoietic responses to hypoxia in renal anemia. Blood 2010, 116:3039−3048
26. Scortegagna M, Ding K, Zhang Q, Oktay Y, Bennett MJ, Bennett M, Shelton JM, Richardson JA, Moe O, Garcia JA: HIF-2alpha regulates murine hematopoietic development in an erythropoietin-dependent manner. Blood 2005, 105:3133−3140
27. Minamishima YA, Kaelin WG Jr.: Reactivation of hepatic EPO synthesis in mice after PHD loss. Science 2010, 329:407
28. Querbes W, Bogorad RL, Moslehi J, Wong J, Chan AY, Bulgakova E, Kuchimanchi S, Akinc A, Fitzgerald K, Koteliansky V, Kaelin WG Jr: Treatment of erythropoietin deficiency in mice with systemically administered siRNA. Blood 2012, 120:1916−1922
29. Yokozawa T, Zheng PD, Oura H, Koizumi F: Animal model of adenine-induced chronic renal failure in rats. Nephron 1986, 44:230−234
30. Ataka K, Maruyama H, Neichi T, Miyazaki J, Gejyo F: Effects of erythropoietin-gene electrotransfer in rats with adenine-induced renal failure. Am J Nephrol 2003, 23:315−323
31. Oyama Y, Hashiguchi T, Taniguchi N, Tancharoen S, Uchimura T, Biswas KK, Kawahara K, Nitanda T, Umekita Y, Lotz M, Maruyama I: High-mobility group box-1 protein promotes granulomatous nephritis in adenine-induced nephropathy. Lab Invest 2010, 90:853−866
32. Tanaka T, Doi K, Maeda-Mamiya R, Negishi K, Portilla D, Sugaya T, Fujita T, Noiri E: Urinary L-type fatty acid-binding protein can reflect renal tubulointerstitial injury. Am J Pathol 2009, 174:1203−1211
33. Postic C, Shiota M, Niswender KD, Jetton TL, Chen Y, Moates JM, Shelton KD, Lindner J, Cherrington AD, Magnuson MA: Dual roles for glucokinase in glucose homeostasis as determined by liver and pancreatic beta cell-specific gene knock-outs using Cre recombinase. J Biol Chem 1999, 274:305−315
34. Smith LE, Wesolowski E, McLellan A, Kostyk SK, D'Amato R, Sullivan R, D'Amore PA: Oxygen-induced retinopathy in the mouse. Invest Ophthalmol Vis Sci 1994, 35:101−111
35. Pierce EA, Avery RL, Foley ED, Aiello LP, Smith LE: Vascular endothelial growth factor/vascular permeability factor expression in a mouse model of retinal neovascularization. Proc Natl Acad Sci USA 1995, 92:905−909
36. Connor KM, Krah NM, Dennison RJ, Aderman CM, Chen J, Guerin KI, Sapieha P, Stahl A, Willett KL, Smith LE: Quantification of oxygen-induced retinopathy in the mouse: a model of vessel loss, vessel regrowth and pathological angiogenesis. Nat Protoc 2009, 4:1565−1573
37. Tomasic NL, Piterkova L, Huff C, Bilic E, Yoon D, Miasnikova GY, Sergueeva AI, Niu X, Nekhai S, Gordeuk V, Prchal JT: The phenotype of polycythemia due to Croatian homozygous VHL (571C>G:H191D) mutation is different from that of Chuvash polycythemia (VHL 598C>T:R200W). Haematologica 2013, 98:560−567
38. Perrotta S, Stiehl DP, Punzo F, Scianguetta S, Borriello A, Bencivenga D, Casale M, Nobili B, Fasoli S, Balduzzi A, Cro L, Nytko KJ, Wenger RH, Della Ragione F: Congenital erythrocytosis associated with gain-of-function HIF2A gene mutations and erythropoietin levels in the normal range. Haematologica 2013, 98: 1624−1632
39. Lanikova L, Lorenzo F, Yang C, Vankayalapati H, Drachtman R, Divoky V, Prchal JT: Novel homozygous VHL mutation in exon 2 is associated with congenital polycythemia but not with cancer. Blood 2013, 121:3918−3924
40. Chen J, Connor KM, Aderman CM, Smith LE: Erythropoietin deficiency decreases vascular stability in mice. J Clin Invest 2008, 118: 526−533
41. Sears JE, Hoppe G, Ebrahem Q, Anand-Apte B: Prolyl hydroxylase inhibition during hyperoxia prevents oxygen-induced retinopathy. Proc Natl Acad Sci USA 2008, 105:19898−19903